0026-895X/01/6006-1343–1348$3.00
MOLECULAR PHARMACOLOGY
Copyright © 2001 The American Society for Pharmacology and Experimental Therapeutics
Mol Pharmacol 60:1343–1348, 2001

Vol. 60, No. 6
1153/946822
Printed in U.S.A.

Molecular Determinants of Inactivation and Dofetilide Block in *ether a-go-go* (EAG) Channels and EAG-Related K^+ Channels

ECKHARD FICKER, WOLFGANG JAROLIMEK,[1] and ARTHUR M. BROWN

Rammelkamp Center for Education and Research, MetroHealth Campus, Case Western Reserve University, School of Medicine, Cleveland, Ohio (E.F., A.M.B.); and I. Physiologisches Institut, Universitaet Heidelberg, Heidelberg, Germany (W.J.)

Received June 13, 2001; accepted September 7, 2001

This paper is available online at http://molpharm.aspetjournals.org

ABSTRACT

The major subunit of the cardiac delayed rectifier current I_{Kr} is encoded by the human *ether a-go-go* related gene (*HERG*). HERG/I_{Kr} channels are blocked selectively by class III antiarrhythmic methanesulfonanilide drugs such as dofetilide. The binding site for methanesulfonanilides is believed to be similar for nonantiarrhythmic drugs such as antihistamines, antibiotics, and antipsychotics. To gain further insight into the binding site, we examined the minimal structural changes necessary to transform low-affinity binding of dofetilide by the related bovine *ether a-go-go* channel bEAG to high-affinity binding of HERG. Previously, it was shown that high-affinity binding in HERG required intact C-type inactivation; the bovine *ether a-go-go* K^+ channel (bEAG), unlike HERG, is noninactivating. Therefore, we introduced C-type inactivation into noninactivating bEAG using site-directed mutagenesis. Two point mutations in the pore region, T432S and A443S, were sufficient to produce C-type inactivation. Low concentrations of dofetilide produced block of bEAG T432S/A443S; unlike HERG, block was almost irreversible. Substitution of an additional amino acid in transmembrane domain S6 made the block reversible. Dofetilide blocked the triply mutated bEAG T432S/A443S/A453S with an IC_{50} value of 1.1 μM. The blocking potency was 30-fold greater than bEAG WT and about one third that of HERG WT. We conclude that high affinity methanesulfonanilide binding to HERG channels is strongly dependent on C-type inactivation.

The hereditary long QT syndrome (LQTS) is caused by mutations in five known genes, four of which encode potassium channel subunits (Keating and Sanguinetti, 2001). Two gene products, KvLQT1 and minK produce α and β subunits of the slowly activating cardiac delayed-rectifier potassium current I_{Ks}. (Wang et al., 1996a; Splawski et al., 1997). The *human ether-a-go-go* related gene HERG (Warmke and Ganetzky, 1994) encodes the major subunit of the rapidly activating cardiac delayed-rectifier potassium channel (Sanguinetti et al., 1995). Mutations in HERG cause chromosome 7-linked LQTS (Curran et al., 1995) and link structural changes in delayed rectifying potassium channels to prolongation of the cardiac action potential, of the QT interval, and of electrocardiogram readings.

HERG K^+ channels have unique pharmacological properties and are blocked with high affinity and selectivity by Class III antiarrhythmic methanesulfonanilides, such as dofetilide, MK-499, and E4031 (Jurkiewicz and Sanguinetti, 1993; Trudeau et al., 1995; Kiehn et al., 1996; Snyders and Chaudhary, 1996; Spector et al., 1996). The binding site that has been proposed (Lees-Miller et al., 2000; Mitcheson et al., 2000b) makes HERG K^+ channels a major target for block by nonantiarrhythmic drugs, including the antihistamines terfenadine (e.g., Roy et al., 1996) and astemizole (Zhou et al., 1999), and the gastrointestinal prokinetic drug cisapride (e.g., Rampe et al., 1997), that cause drug-induced LQTS as an unwanted side effect.

Previous structure-function studies of high-affinity drug binding in HERG K^+ channels provided evidence that intact C-type inactivation is crucial for drug binding, because many mutations that disrupted inactivation dramatically reduced the sensitivity to methanesulfonanilide drugs, most probably because of allosteric changes induced in the drug binding site (Wang et al., 1997b; Ficker et al., 1998; Herzberg et al., 1998; Lees-Miller et al., 2000). Similarly, it has been demonstrated that high-affinity drug binding can be modulated by extracellular cations such as K^+, Na^+, or Cd^{2+}, all of which modify inactivation gating of HERG K^+ channels (Wang et al., 1997; Numaguchi et al., 2000).

This study was supported by a Grant-in-aid award from the American Heart Association, Northeast Ohio Affiliate, Inc (to E.F.); and by National Institutes of Health Grants HL61642, HL36930 and DK54178 (to A.M.B.).

[1] Present address: Merck Sharp and Dohme Research Laboratories, Neuroscience Research Center, Harlow, Essex, UK.

ABBREVIATIONS: LQTS, long QT syndrome; I_{Kr}, cardiac delayed rectifier; dofetilide, *N*-[4-(-{-[4-(methanesulfonamino)-phenoxyl]-*N*-methylethylamino}ethyl)phenyl]methanesulfonamide; HERG, human *ether a-go-go* related gene; MK-499, (+)-*N*-[1′-(6-cyano-1,2,3,4-tetrahydro-2(*R*)-naphthalenyl)-3,4-dihydro-4(*R*)-hydroxyspiro(2*H*-1-benzopyran-2,4′-piperidin)-6-yl]methanesulfonamide] monohydrochloride; bEAG, bovine *ether a-go-go* K^+ channel; WT, wild-type; TEA, tetraethylammonium.

Major progress toward a structural basis of high-affinity drug binding has recently been made with the identification of two crucial aromatic amino acid residues in the S6 transmembrane domain of the channel protein: HERG Y652 and F656. These two amino acids seem to constitute a major part of the methanesulfonanilide binding site in HERG with additional contributions being made by residue G648 in S6 and residues T623 and V625 in the pore helix of the HERG channel protein (Lees-Miller et al., 2000; Mitcheson et al., 2000b). These residues face the conduction pathway, and are accessible only in the open state and drug molecules are trapped inside the conduction pathway by closure of the activation gate (Mitcheson et al., 2000a,b).

With localization of the receptor for high-affinity drug binding to the S6 transmembrane domain, the role played by C-type inactivation in enhancing drug binding is problematic for the following reasons: 1) mutations such as HERG S620T, in which inactivation has been completely removed, showed dramatically lowered drug-sensitivity despite the availability of F656 and Y652 (Ficker et al., 1998); 2) all residues important for drug binding are conserved in the closely related, noninactivating EAG K^+ channels yet EAG channels are relatively insensitive to block by dofetilide or MK-499 (Ficker et al., 1998; Herzberg et al., 1998; Mitcheson et al., 2000b); 3) mutations at several of the binding loci (e.g., HERG G648A, T623A, F656A) showed a large negative shift in inactivation (i.e., increased inactivation); contrary to expectations, however, they were less sensitive to drug block than WT channels (Mitcheson et al., 2000b); and 4) some mutations that completely removed inactivation remained rather sensitive to methanesulfonanilide block (e.g., HERG S620C or HERG G628C/S631C; Wang et al., 1997; Ficker et al., 1998; Mitcheson et al., 2000b). These inconsistencies show that the interaction between inactivation and the pore lining residues implicated in drug binding is not understood.

In the present experiments, we examined this interaction by addressing the difference in drug sensitivity between HERG and EAG channels. We mutated the noninactivating EAG family member bEAG, which is about 100-fold less sensitive to dofetilide than HERG, by substitution of two amino acids at positions 432 and 443 in the pore region. These mutations introduced HERG-like C-type inactivation and high-affinity dofetilide binding simultaneously. However, block by dofetilide was almost irreversible, even at low concentrations, unlike the situation in HERG. To convert bEAG T432S/A443S into a channel that was blocked reversibly by dofetilide, we mutated one additional residue in the S6 transmembrane helix. Taken together, our results show that introducing C-type inactivation into bEAG was sufficient to transform the low affinity methanesulfonanilide binding site of bEAG into a high-affinity site resembling HERG channels.

Materials and Methods

Construction of Mutant Channels. HERG WT cDNA was a gift from Dr. M. T. Keating (University of Utah, Salt Lake City, UT). bEAG WT cDNA was provided by Dr. A. Baumann (Forschungszentrum Juelich, Juelich, Germany). All point mutations in HERG and bEAG were generated by overlap extension polymerase chain reactions using polymerase chain reaction-generated *Mlu*I-*Kpn*I cassettes anchored in pBluescript as template (Ficker et al., 1998). Before subcloning, the cassettes were sequenced. cRNA was prepared using the mMessage mMachine in vitro transcription kit (Ambion, Austin, TX) and SP6 polymerase after linearization with *Eco*RI (HERG WT, and point mutations in HERG) or *Eco*RV (bEAG WT, and point mutations in bEAG).

Electrophysiology. Isolation, maintenance, and injection of *Xenopus laevis* oocytes were performed as described previously (Ficker et al., 1998). Whole-cell currents were recorded 2 to 7 days after cRNA injection using standard two-microelectrode voltage clamp techniques. Bath solutions were 96 mM NaCl, 5 mM KCl, 1.8 mM $CaCl_2$, 1.0 mM $MgCl_2$, 5 mM HEPES (5K Ringer, pH 7.4) and 1.8 mM $CaCl_2$, 10 mM HEPES with either 115 mM KCl (115K Ringer, pH 7.4), 115 mM RbCl (115Rb Ringer, pH 7.4), 115 mM CsCl (115Cs Ringer, pH 7.4), or 115 mM NaCl (115Na Ringer, nominally K^+-free, pH 7.4). Bath solutions containing 100 mM $[K]_{ex}$, 30 mM $[K]_{ex}$, and 5 mM $[K]_{ex}$ with 30 mM TEA added were prepared by equivalent reductions in the concentration of NaCl in 5K Ringer or by omission of KCl for a nominally K^+-free 100Na Ringer. For IC_{50} measurements, dofetilide was perfused in increasing concentrations with 5K Ringer. Dofetilide was provided by Pfizer Central Research (Groton, CT). All other chemicals were obtained from Sigma (St. Louis, MO). Macropatch recordings were performed using an EPC-7 patch clamp amplifier (List, Darmstadt, Germany). Patch pipettes had resistances of 0.2 to 0.6 MΩ and were filled with 5K Ringer (see above). For patch recordings the bath solution had the following composition: 100 mM KCl, 5 mM EDTA, 5 mM EGTA, 10 mM HEPES (isoK, pH 7.4). No leak subtraction was applied. All recordings were performed at room temperature (20–22°C). pClamp software (Axon Instruments, Foster City, CA) was used for the generation of voltage clamp pulses and for data acquisition. When appropriate, data were expressed as mean ± S.E.M.

Results

Pore Mutations That Introduce C-Type Inactivation in bEAG. Several reports have shown that amino acid residues in positions 620 and 631 are crucial for C-type inactivation in HERG channels (Schoenherr and Heinemann, 1996; Smith et al., 1996; Ficker et al., 1998; Herzberg et al., 1998). To introduce C-type inactivation in bEAG, we placed serines at position 432 or 443 of bEAG because these positions are equivalent to S620 and S631 in HERG. Neither bEAG A443S nor bEAG T432S introduced the inactivating current phenotype that was desired (Ficker et al., 1998).

However, a combination of the two point mutations bEAG T432S and A443S successfully introduced the desired phenotype. With depolarizing voltage commands, a rapidly activating and inactivating outward current was elicited (Fig. 1A). The current-voltage relationship was bell-shaped (Fig. 1B). Deactivation of the tail currents was also rapid. Current inactivation persisted after excision of the membrane patch into divalent and Na^+-free isoK$^+$ Ringer solution (Fig. 1C). In cell-attached macropatches, currents decayed monoexponentially. Time constants were voltage-dependent with 24.5 ± 1.7, 19.3 ± 1.0, and 15.5 ± 1.1 ms (n = 6) measured at membrane potentials of −20, 0, and +20 mV, respectively. These values were about double the time constants measured in macropatch recordings of HERG WT. In HERG, time constants were 12.4 ± 0.6, 10.6 ± 0.5, and 7.4 ± 0.6 ms at −20, 0, and +20 mV, respectively (n = 6). The difference in time constants may be related to the different voltage protocols that were used. In bEAG T432S/A443S, we analyzed current inactivation using depolarizing voltage commands at which channel activation and inactivation proceeded simultaneously (Fig. 1A). In HERG, a three-step pulse protocol was used that isolated inactivation from activation (Smith et al.,

1996). For similar reasons, fractional inactivation differed between the two channels. At more hyperpolarized membrane potentials, at which current activation was slow, bEAG T432S/A443S currents seemed to inactivate much less than HERG WT currents. At more depolarizing potentials, however, at which activation was considerably faster, fractional inactivation approached the values measured for HERG WT channels. In marked contrast, the inactivation process in HERG S631A was shifted to more positive values (Fig. 1D; see Zou et al., 1998). In addition, the time course for recovery from inactivation was equally fast in bEAG T432S/A443S and HERG WT. At −80 mV, the time constant for recovery from inactivation was 17.1 ± 2.1 ms (n = 4; Fig. 1E) and is comparable with the time constant of about 10 ms measured at −80 mV for HERG WT (Sanguinetti et al., 1995).

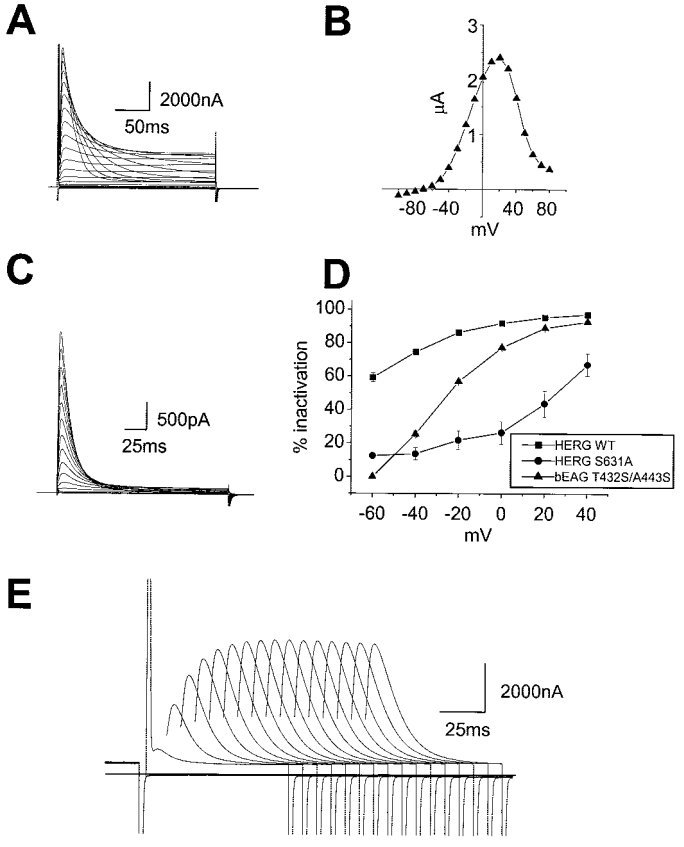

Fig. 1. Introduction of C-type inactivation in bEAG. A, bEAG T432S/A443S currents, two-microelectrode, voltage-clamp recording in an *X. laevis* oocyte. Depolarizing test pulses from −100 to +80 mV in 10 mV increments, holding potential, −80 mV. B, Current-voltage relationship measured at the end of test pulses for recordings shown in A. C, inside-out macropatch recording in isoK-Ringer. Depolarizing test pulses from −90 to +80 mV in 10-mV increments; holding potential, −80 mV. $[K^+]_{pipette}$ was 5 mM. D, comparison of fractional inactivation of HERG WT (■), HERG S631A (●), and bEAG T432S/A443S (▲), n = 5 to 7. Fractional inactivation was calculated in two-microelectrode recordings from peak and steady-state currents elicited with pulse protocols as shown in A for bEAG T432S/A443S. For HERG WT and HERG S631A, fractional inactivation was analyzed using instantaneous current-voltage protocols with test pulses following directly on 25- or 4-ms steps to −100 mV to remove inactivation. E, recovery from inactivation in bEAG T432S/A443S. A double pulse protocol with test pulses to +50 mV was used to assess removal of inactivation. Between test pulses, membrane potential was stepped for variable durations to −80 mV to progressively remove inactivation; holding potential, −80 mV. Positive-going capacitive transients have been blanked for clarity. Two-microelectrode recordings were done in 5 mM $[K^+]_{ex}$. Dashed lines indicate zero current level.

To demonstrate that C-type inactivation was introduced into bEAG K^+ channels, we tested the effects of extracellular TEA, elevated $[K^+]_{ex}$, and various extracellular monovalent cations known to interfere with C-type inactivation (Choi et al., 1991; Lopez-Barneo et al., 1993; Schoenherr and Heinemann, 1996). TEA at 30 mM blocked bEAG channels by about 50% and produced the expected slowing of inactivation over a wide range of potentials (Fig. 2, A and B). Likewise, inactivation was slowed by elevated $[K^+]_{ex}$ that at the same time increased current amplitude (Fig. 2, C and D). Moreover, in high K^+, it was apparent that the tail currents of bEAG T432S/A443S no longer deactivated almost instantaneously. Deactivation of tail currents was slowed sufficiently that recovery from inactivation produced a clearly resolved rising phase in inward tail currents that in HERG WT channels was attributed to recovery from C-type inactivation. In many potassium channels slowing of C-type inactivation by extracellular cations followed the selectivity sequence for permeation, namely $K^+ \sim Rb^+ > Cs^+ > Na^+$ (Lopez-Barneo et al., 1993). We found that inactivation in bEAG T432S/A443S was slowed most with Rb^+ and Cs^+ following the

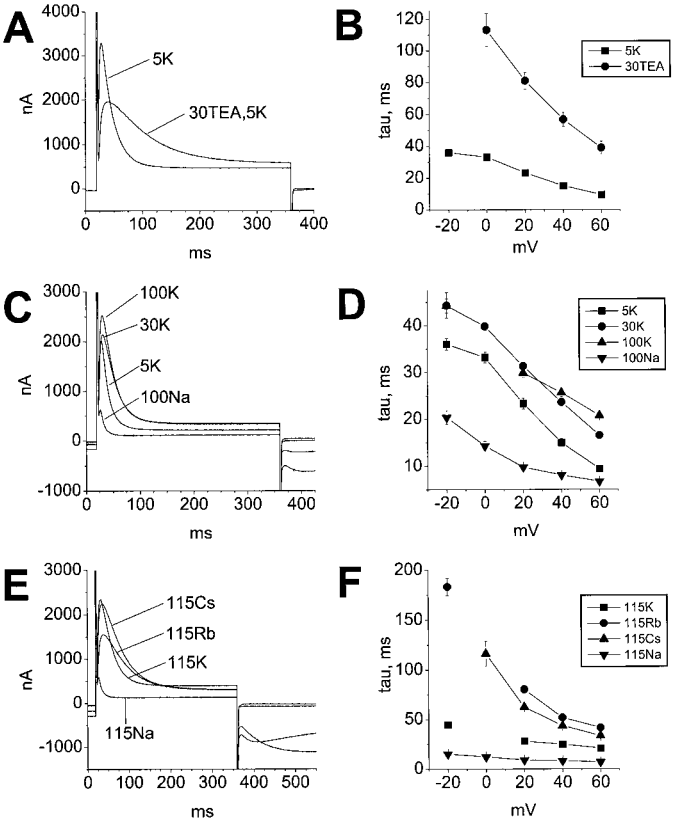

Fig. 2. Effects of TEA, extracellular potassium and monovalent cations on inactivation kinetics of bEAG T432S/A443S. Current traces shown in A, C, and E were elicited with test pulses to 40 mV from a holding potential of −90 mV. A, effect of 30 mM TEA in 5K Ringer. External TEA slows time course of current inactivation. B, time constants of inactivation in 5K Ringer (■) and 5K Ringer + 30 mM TEA (●) as a function of membrane potential; n = 7 to 8. C, effect of $[K]_{ex}$ on inactivation kinetics. Increasing $[K]_{ex}$ slows time course of inactivation. 100Na refers to a solution nominally free of K^+. D, time constants in different $[K]_{ex}$: 5K (■), 30K (●), 100K (▲), and 100Na (0K, ▼); n = 5 to 8. E, effects of 115K^+, Rb^+, Cs^+, and Na^+ on current inactivation. F, time constants with different monovalent cations in bath solution: 115K (■), 115Cs (▲), 115Rb (●), and 115Na (0K, ▼); n = 4. All current decays were fitted with monoexponential functions.

sequence $Rb^+ \geq Cs^+ > K^+ > Na^+$ (Fig. 2, E and F). As for HERG channels, inactivation in bEAG T432S/A443S was strongly voltage-dependent (Wang et al., 1996b).

Dofetilide Block of bEAG T432S/A443S. Intact C-type inactivation has been shown to be a prerequisite for high-affinity binding of methanesulfonanilide drugs in HERG K^+ channels (Wang et al., 1997; Ficker et al., 1998; Herzberg et al., 1998). Consequently, single point mutations at bEAG 432 or bEAG 443 that express noninactivating currents failed to produce high-affinity drug binding in bEAG. BEAG T432S resulted in a channel only 4-fold more sensitive to dofetilide than bEAG WT, whereas bEAG A443S currents were slightly less sensitive than WT currents (Table 1).

In contrast, inactivating bEAG T432S/A443S channels provided a unique tool to ask whether introduction of C-type inactivation is sufficient to convert the low-affinity binding site of bEAG into the high-affinity site of HERG. Block by methanesulfonanilides was evaluated in two-microelectrode recordings with a prepulse protocol to accelerate onset of block. Figure 3 shows bEAG T432S/A443S currents recorded at 0 mV during perfusion of 1 μM dofetilide. Onset of block was slow and a well-defined steady-state level was not always attained. Moreover, drug block was almost irreversible, even after prolonged washout of more than 1 h (Figs. 3 and 4D). To obtain estimates of dofetilide block in bEAG T432S/A443S, we added 0.3 and 1 μM dofetilide to the extracellular perfusate and extrapolated steady-state block by monoexponential fits to the time course of amplitude reductions. Dofetilide (1 μM) reduced current amplitudes to 20 $\pm$ 4% of control levels (n = 13). With 0.3 μM dofetilide, currents were on average reduced to 38 $\pm$ 2% (n = 3). For comparison, the block of HERG WT currents at 0 mV by 1 μM dofetilide was superimposed on the time-dependent block of bEAG T432S/A443S in Fig. 3. The onset of block in HERG was much faster and the drug effects were reversible. On the other hand, bEAG WT was insensitive to dofetilide at this concentration. Although a precise IC_{50} value could not be measured in bEAG T432S/A443S, our experiments indicate that fairly low concentrations of dofetilide significantly block bEAG T432S/A443S currents with an $IC_{50} < 1$ μM. By contrast, the IC_{50} in bEAG WT is 32 μM (Table 1).

An explanation for the irreversible drug block in bEAG T432S/A443S may be trapping of dofetilide in the inner vestibule by a rapidly closing activation gate. In HERG channels, recovery from block is slow because of trapping by a gate that closes much more slowly than in bEAG T432S/A443S (Mitcheson et al., 2000a). Trapping of dofetilide in bEAG T432S/A443S channels could be tested directly by the introduction of additional mutations that either slow deactivation or induce reopenings at negative membrane potentials as described for HERG D540K (Sanguinetti and Xu, 1999). Along these lines, we described previously a HERG/EAG chimera with bEAG S6 transplanted into HERG background (HBS6; Ficker et al., 1998) that expressed a nonfunctional, permanently opened activation gate combined with fully preserved C-type inactivation. HBS6 channels were more sensitive to block by dofetilide than HERG WT channels with drug block being reversible.

To quantify the increased sensitivity of bEAG channels to dofetilide upon introduction of C-type inactivation, in the present study, we engineered additional mutations in the bEAG T432S/A443S background to achieve reversible blockade and measure half-maximal blocking concentrations. We focused on two positions in the N-terminal half of S6 at which hydrophilic S641 and C643 residues of HERG were represented by hydrophobic A453 and A455 residues in bEAG. bEAG T432S/A443S+A455C showed the behavior of bEAG T432S/A443S with respect to kinetics, C-type inactivation, and irreversible dofetilide binding (data not shown). In contrast, bEAG T432S/A443S+A453S activated slowly at potentials more negative than 20 mV and exhibited no detectable inactivation. At potentials more depolarized than 20 mV, however, channels inactivated and produced a crossover of raw current traces (Fig. 4A). The current-voltage relationship was bell-shaped (Fig. 4B) and voltage-dependent inactivation was apparent when the holding potential was shifted from -80 to -60 mV to accelerate current activation (Fig. 4A, inset). Onset of dofetilide block was slow, but in contrast

TABLE 1

Comparison of dofetilide block between HERG and bEAG mutants

Concentration-response relationships were fit with Hill equations according to a one-to-one binding scheme (Hill coefficient n = 1). Fits to concentration response curves in bEAG WT assume the same binding scheme. However, better fits could be obtained with Hill coefficients of about 0.6.

	IC_{50}	n
	μM	
HERG WT[a]	0.32 $\pm$ 0.04	24
bEAG T432S/A443S/A453S	1.1 $\pm$ 0.2	7
bEAG T432S/A443S	<1	13
bEAG T432S[a]	7.8 $\pm$ 1.2	5
bEAG WT[a]	31.8 $\pm$ 7.5	6
bEAG A443S[a]	41.8 $\pm$ 5.0	5

[a] Ficker et al. (1998).

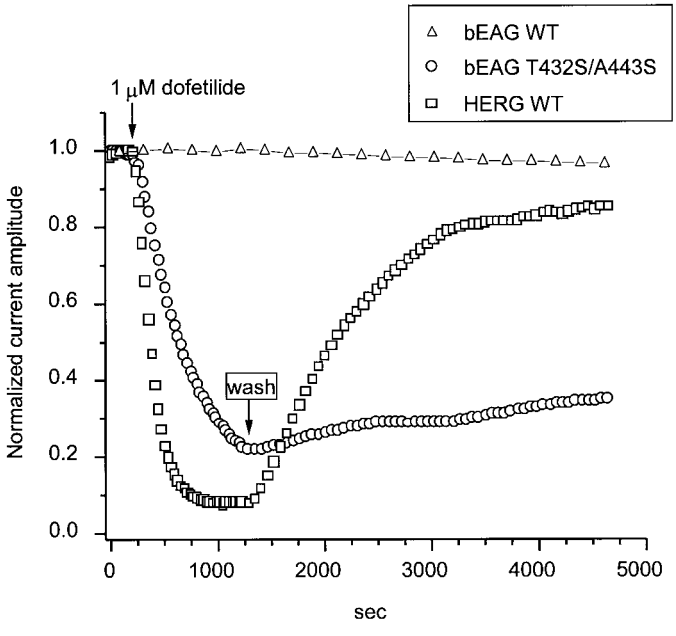

Fig. 3. Sensitivity and time dependence of dofetilide block in bEAG T432S/A443S. Two-microelectrode, voltage-clamp recordings; holding potential, -80 mV; 1600-ms test pulse to 0 mV preceded by 20 conditioning 400-ms prepulses to 0 mV applied at 1Hz; 5K Ringer. Shown are steady-state currents measured at the end of test pulse to 0 mV. Slow time-dependent block of BEAG T432S/A443S (○) by 1 μM dofetilide. Only partial washout could be obtained. For comparison, time-dependent dofetilide block of bEAG WT (△) and HERG WT (□) is shown. In contrast to bEAG T432S/A443S, 80 to 100% of control values could be recovered in HERG WT during washout.

to bEAG T432S/A443S, a steady state was reached within several minutes. The block was now reversible; Fig. 4D shows the washout after the application of 10 μM dofetilide, which blocked currents by about 90%. The time course of recovery from block could be approximated by monoexponential functions with a mean time constant of 673 ± 53 s (n = 7). On average, 72 ± 6% of control currents were recovered (n = 8). The washout kinetics of bEAG T432S/A443S/A453S were considerably slower than the time constant of 99 ± 9.8 s measured in bEAG WT after application of 100 μM dofetilide that blocked bEAG WT by about 90% (n = 11). The recovery time constant of HERG-WT was 1450 ± 226 s (with 10 μM dofetilide) and was about double the time constant of bEAG T432S/A443S/A453S. For comparison, the extremely slow wash out kinetics of bEAG T432S/A443S is given in Fig. 4D. The differences in rates of recovery from 90% drug block in bEAG WT, bEAG T432S/A443S/A453S, and HERG WT correlated with differences in IC_{50} values. In bEAG T432S/A443S/A453S, the IC_{50} value of dofetilide block was 1.1 ± 0.2 μM (n = 7, Fig. 4C and Table 1). This channel construct was about 30-fold more sensitive to dofetilide than bEAG WT (IC_{50}, 31.8 ± 7.5 μM, n = 6) and only about 3-fold less sensitive than HERG WT (IC_{50}, 0.32 ± 0.04 μM, n = 24).

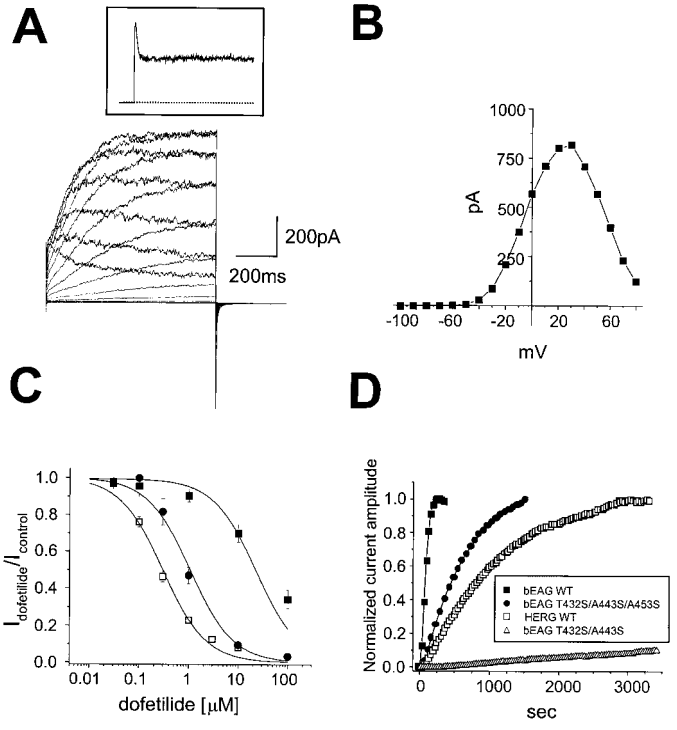

Fig. 4. Additional mutation in S6 alters dofetilide binding. A, triple mutant bEAG T432S/A443S/A453S currents, cell-attached macropatch recording. Depolarizing test pulses from −100 to +80 mV in 10 mV increments; holding potential, −80 mV. $[K^+]_{pipette}$ was 5 mM. Inset, inactivating current component elicited with a depolarizing test pulse to +60 mV from a holding potential of −60 mV. B, current-voltage relationship measured at the end of test pulses for recordings shown in A. C, two-microelectrode, voltage-clamp recordings were used to assess dofetilide block: holding potential, −80 mV; 1600-ms test pulse to 0 mV preceded by 20 conditioning prepulses to 0 mV applied at 1Hz. Current amplitudes were measured at the end of test pulses to 0 mV. $[K^+]_{ex}$ was 5 mM. Concentration response relationships for HERG WT (open squares), bEAG WT (closed squares) and bEAG T432S/A443S/A453S (●) were fitted with Hill equations according to a one-to-one binding scheme (Hill coefficient, n = 1). Solid lines show fit to data points with Hill equations of the form: $I_{dofetilide} / I_{control} = 1 / [1 + (D / IC_{50})^{nH}]$, where D is dofetilide concentration, n_H is the Hill coefficient, and IC_{50} is the concentration necessary for 50% block (Table 1). D, normalized washout kinetics of dofetilide block in bEAG WT (after application of 100 μM dofetilide, ■), HERG WT (after the application of 10 μM dofetilide, □), bEAG T432S/A443S/A453S (after 10 μM dofetilide, ●) and bEAG T432S/A443S (after 100 μM dofetilide, △). Washout was monitored with pulse protocol described in C.

Discussion

Mapping the binding site for dofetilide in HERG channels is complicated by tight coupling between binding and C-type inactivation. To complement experiments done with "loss of function" mutations in HERG, we adopted a "gain of function" strategy in bEAG and showed that mutation of two amino acid residues in the pore region introduced C-type inactivation and high-affinity dofetilide binding.

Successful transfer of C-type inactivation into bEAG relied upon the analysis of structural inactivation determinants in HERG. In general, C-type inactivation is sensitive to mutations in or close to the pore region (e.g., Hoshi et al., 1991; Lopez-Barneo et al., 1993). C-type inactivation in HERG was altered by mutating position 631, a pore residue homologous to Shaker 449 in the external mouth of the pore (Schoenherr and Heinemann, 1996). Mutation of HERG S620 to T620, a residue located at the inner end of the pore helix and not exposed to the conduction pathway as judged from Doyle et al. (1998) had even more pronounced effects, completely abolishing C-type inactivation (Ficker et al., 1998; Herzberg et al., 1998). Interestingly, HERG S620 is homologous to position 369 in Kv2.1, a residue with large effects on current inactivation (DeBiasi et al., 1993). These results raise the question of how residues facing opposite sites of the membrane are involved in C-type inactivation. HERG S631 localizes to the external mouth of the pore and by analogy with Shaker 449 is believed to control access of external ions to a more internally located C-type inactivation site (Molina et al., 1997). HERG S620 might affect C-type inactivation by contributing to ion occupancy at a critical site in the selectivity filter as demonstrated for Shaker A463C (Ogielska and Aldrich, 1999). The proposition that both HERG620 and HERG631 regulate ion occupancy at the C-type inactivation site (Herzberg et at., 1998), is further supported by our results with reverse mutations in bEAG. Neither bEAG T432S nor bEAG A443S alone expressed C-type inactivating currents, whereas the combination of both mutations in bEAG T432S/A443S introduced an inactivation process with the hallmarks of C-type inactivation.

Given the tight coupling between C-type inactivation and high-affinity drug binding in HERG, our results showed, not unexpectedly, that C-type inactivating bEAG T432S/A443S and bEAG T432S/A443S/A543S channels were blocked by low concentrations of dofetilide. Previous work in Shaker K^+ channels suggested that conformational changes of C-type inactivation were restricted to the selectivity filter (Liu et al., 1996; Molina et al., 1997; Harris et al., 1998). By contrast, critical structural determinants for high-affinity drug binding in HERG have been located to positions 652 and 656 in the S6 transmembrane domain, positions that are conserved in EAG channels (Lees-Miller et al., 2000; Mitcheson et al., 2000). How, then, can C-type inactivation communicate with a drug-binding site controlled by S6 residues facing the internal vestibule and conduction pathway? One possibility is that C-type inactivation interacts with a rotational move-

ment of S6 during activation making crucial residues in S6 accessible for drug binding. In the closed state of the HERG channel, these residues are hidden consistent with the absence of resting block by methanesulfonanilides (Kiehn et al., 1996; Snyders and Chaudhary, 1996). In Shaker channels, it has been shown that small changes in the size of a side chain (Shaker I470C) allow blockers suddenly to become trapped in the closed state of the channel protein; it has been suggested that structural differences between channels that do and do not trap blockers are only minor (Holmgren et al., 1997). Therefore, it is conceivable that point mutations affecting C-type inactivation may change the size of the internal vestibule of channels in the EAG gene family and thereby allow or impede trapping of methanesulfonanilides. Because trapping of high-affinity blockers has important consequences for the reversibility of block in HERG channels leading to accumulation of drug effects, it may be important in future experiments to determine the relationship between inner vestibule size, C-type inactivation, and drug binding more precisely to develop new blocking molecules that might escape from their binding sites more readily.

Acknowledgments

We thank Dr. M. T. Keating for the HERG cDNA clone; Dr A. Baumann for the bEAG cDNA clone; T. Carroll and Dr. W.-Q. Dong for expert technical assistance; Dr. B. Wible for help with some of the mutations; and Dr. G. Kirsch for helpful comments on the manuscript.

References

Choi KL, Aldrich RW, and Yellen G (1991) Tetraethylammonium blockade distinguishes two inactivation mechanisms in voltage-activated K^+ channels. *Proc Natl Acad Sci USA* **88:**5092–5095.

Curran ME, Splawski I, Timothy KW, Vincent GM, Green ED, and Keating MT (1995) A molecular basis for cardiac arrhythmia: HERG mutations cause long QT syndrome. *Cell* **80:**795–804.

DeBiasi M, Hartmann HA, Drewe JA, Taglialatela M, Brown AM, and Kirsch GE (1993) Inactivation determined by a single site in K^+ pores. *Pfleug Arch Eur J Physiol* **422:**354–363.

Doyle DC, Morais Cabral J, Pfuetzner RA, Kuo A, Gulbis JM, Cohen SL, Chait BT, and MacKinnon R (1998) The structure of the potassium channel: molecular basis of K^+ conduction and selectivity. *Science (Wash DC)* **280:**69–77.

Ficker E, Jarolimek W, Kiehn J, Baumann A, and Brown AM (1998) Molecular determinants of dofetilide block of HERG K^+ channels. *Circ Res* **82:**386–395.

Harris RE, Larsson HP, and Isacoff EY (1998) A permeant ion binding site located between two gates of the Shaker K^+ channel. *Biophys J* **74:**1808–1820.

Herzberg IM, Trudeau MC, and Robertson GA (1998) Transfer of rapid inactivation and sensitivity to the class III antiarrhythmic drug E-4031 from HERG to M-eag channels. *J Physiol (Lond)* **511:**3–14.

Holmgren M, Smith PL, and Yellen G (1997) Trapping of organic blockers by closing of voltage-dependent K^+ channels: evidence for a trap door mechanism of activation gating. *J Gen Physiol* **109:**527–535.

Hoshi T, Zagotta WN, and Aldrich RW (1991) Two types of inactivation in Shaker K^+ channels: effects of alterations in the carboxy-terminal region. *Neuron* **7:**547–556.

Jurkiewicz NK and Sanguinetti MC (1993) Rate-dependent prolongation of cardiac action potentials by a methanesulfonanilide class III antiarrhythmic agent. *Circ Res* **72:**75–83.

Keating MT and Sanguinetti MC (2001) Molecular and cellular mechanisms of cardiac arrhythmias. *Cell* **104:**569–580.

Kiehn J, Lacerda AE, Wible BA, and Brown AM (1996) Molecular physiology and pharmacology of HERG. *Circulation* **94:**2572–2579.

Lees-Miller JP, Duan Y, Teng GQ, and Duff HJ (2000) Molecular determinants of high-affinity dofetilide binding to HERG1 expressed in *Xenopus* oocytes: involvement of S6 sites. *Mol Pharmacol* **57:**367–374.

Liu Y, Jurman ME, and Yellen G (1996) Dynamic rearrangement of the outer mouth of a K^+ channel during gating. *Neuron* **16:**859–867.

Lopez-Barneo J, Hoshi T, Heinemann SH, and Aldrich RW (1993) Effects of external cations and mutations in the pore region on C-type inactivation of Shaker potassium channels. *Recept Channels* **1:**61–71.

Mitcheson JS, Chen J, and Sanguinetti MC (2000a) Trapping of a methanesulfonanilide by closure of the HERG potassium channel activation gate. *J Gen Physiol* **115:**229–240.

Mitcheson JS, Chen J, Lin M, Culberson C, and Sanguinetti MC (2000b) A structural basis for drug-induced long QT syndrome. *Proc Natl Acad USA* **97:**12329–12333.

Molina A, Castellano AG, and Lopez-Barneo J (1997) Pore mutations in Shaker K^+ channels distinguish between the sites of tetraethylammonium blockade and C-type blockade. *J Physiol (Lond)* **499:**361–367.

Numaguchi H, Mullins FM, Johnson JPJ, Johns DC, Po SS, Yang ICH, Tomaselli GF, and Balser JR (2000) Probing the interaction between inactivation gating and d-sotalol block of HERG. *Circ Res* **87:**1012–1018.

Ogielska EM and Aldrich RW (1999) Functional consequences of a decreased potassium affinity in a potassium channel pore. *J Gen Physiol* **113:**347–358.

Rampe D, Roy M, Dennis A, and Brown AM (1997) A mechanism for the proarrhythmic effects of cisapride (Propulsid): high affinity blockade of the human cardiac potassium channel HERG. *FEBS* **417:**28–32.

Roy M, Dumaine R, and Brown AM (1996) HERG, a primary human ventricular target of the nonsedating antihistamine terfenadine. *Circulation* **94:**817–823.

Sanguinetti MC, Jiang C, Curran ME, and Keating MT (1995) A mechanistic link between an inherited and an acquired cardiac arrhythmia: HERG encodes the I_{Kr} potassium channel. *Cell* **81:**299–307.

Sanguinetti MC and Xu QP (1999) Mutations of the S4–S5 linker alter activation properties of HERG potassium channels expressed in *Xenopus* oocytes. *J Physiol (Lond)* **514:**667–675.

Schoenherr R and Heinemann SH (1996) Molecular determinants for activation and inactivation of HERG, a human inward rectifier potassium channel. *J Physiol (Lond)* **493:**635–642.

Smith PL, Baukrowitz T, and Yellen G (1996) The inward rectification mechanism of the HERG cardiac potassium channel. *Nature (Lond)* **379:**833–836.

Snyders DJ and Chaudhary A (1996) High affinity open channel block by dofetilide of HERG expressed in a human cell line. *Mol Pharmacol* **49:**949–955.

Spector PS, Curran ME, Keating MT, and Sanguinetti MC (1996) Class III antiarrhythmic drugs block HERG, a human cardiac delayed rectifier K+ channel. Open-channel block by methanesulfonanilides. *Circ Res* **78:**499–503.

Splawski I, Tristani-Firouzi M, Lehamnn MH, Sanguinetti MC, and Keating MT (1997) Mutations in the hminK gene cause long QT syndrome and suppress Iks function. *Nat Genet* **17:**338–340.

Trudeau MC, Warmke JW, Ganetzky B, and Robertson GA (1995) HERG, a human inward rectifier in the voltage-gated potassium channel family. *Science (Wash DC)* **269:**92–95.

Wang Q, Curran ME, Splawski I, Burn TC, Millholland JM, VanRaay TJ, Shen J, Timothy KW, Vincent GM, de Jager T, et al. (1996a) Positional cloning of a novel potassium channel gene: KvLQT1 mutations cause cardiac arrhythmias. *Nat Genet* **12:**17–23.

Wang S, Morales MJ, Liu S, Strauss HC, and Rasmusson RL (1996b) Time, voltage and ionic concentration dependence of rectification of h-erg expressed in *Xenopus* oocytes. *FEBS Lett* **389:**167–173.

Wang S, Morales MJ, Liu S, Strauss HC, and Rasmusson RL (1997) Modulation of HERG affinity for E-4031 by $[K^+]_o$ and C-type inactivation. *FEBS Lett* **417:**43–47.

Warmke JW and Ganetzky B (1994) A family of potassium channel genes related to eag in *Drosophila* and mammals. *Proc Natl Acad USA* **91:**3438–3442.

Zhou Z, Vorperian VR, Gong Q, Zhang S, and January CT (1999) Block of HERG potassium channels by the antihistamine astemizole and its metabolites desmethylastemizole and norastemizole. *J Cardiovasc Electrophysiol* **10:**836–843.

Zou A, Xu QP, and Sanguinetti MC (1998) A mutation in the pore region of HERG K^+ channels expressed in *Xenopus* oocytes reduces rectification by shifting the voltage dependence of inactivation. *J Physiol (Lond)* **509:**129–137.

Address correspondence to: Dr. Eckhard Ficker, Rammelkamp Center, MetroHealth Medical Center, 2500 MetroHealth Drive, Cleveland, OH 44109-1998. E-mail: eficker@metrohealth.org